JMEPEG (2009) 18:312–318
DOI: 10.1007/s11665-008-9290-9

1059-9495/$19.00

Interfacial Bonding Strength Between Brazing Alloys and CVD Diamond

Yu-Chan Hsieh and Shun-Tian Lin

(Submitted October 7, 2007; in revised form July 2, 2008)

Three groups of brazing alloys were compared in brazing chemical-vapor-deposited (CVD) diamond, including two nickel-based alloys (Ni-3Fe-7Cr-3B-0.5Si-0.02C and Ni-14Cr-10P-0.02C), one copper-based alloy (Cu-10Sn-15Ti), and two silver-based alloys (Ag-5Cu-1Al-1.25Ti and Ag-34.25Cu-1In-1.75Ti). The nickel-based alloys catalytically transformed the sp^3-bonded diamond into sp^2-bonded carbon during high-temperature brazing operation though with the existence of Cr as the active metal. The bonding strength was very low and the fracture primarily propagated through the sp^2-bonded carbon. For Cu-10Sn-15Ti brazing alloy, the transformation of the sp^3-bonded diamond into sp^2-bonded carbon during high-temperature brazing operation was marginal. The bond strength was adequate and fracture took place primarily through the brazing alloy bulk, due to the high concentrations of Sn and Ti that caused the precipitation of abundant intermetallic compounds in the brazing alloy bulk. For Ag-based alloys having very low concentrations of Ti, no visible degradation of diamond was observed and the bonding strength was very high. Crack primarily propagated through the brazed interface or even the CVD diamond bulk.

Keywords brazing, heat treating, joining, material selection

1. Introduction

Brazing chemical-vapor-deposited (CVD) diamond onto different substrates is a practice that facilitates the widespread applications of expensive diamond. Different brazing alloy systems have been proposed (Ref 1-3), which can be categorized into three main groups, including Ni-, Cu-, and Ag-based alloys. The brazing alloys are mainly composed of a main composition, a melting temperature depressor, and an active metal. The active metals are expected to enhance the interfacial bonding strength by developing an intermediate carbide layer that alleviates the interfacial stresses arising from the difference in bond type and lattice parameter, and the phase change of the brazing alloy subsequent to brazing operation (Ref 1, 3).

Table 1 shows the brazing temperatures of various Ni-, Cu-, and Ag-based alloys, which were used to braze diamond (Ref 1, 2, 4-12). The Ni-based alloys are mainly composed of a large quantity of Cr as the active metal and B or P as the melting temperature depressor (Ref 13). Due to the inherent nature of high eutectic temperatures, the Ni-based alloys usually have a brazing operation temperature higher than 1000 °C. An interfacial carbide phase layer, composed of Cr_3C_2, Cr_7C_3, and $Cr_{23}C_6$, was typically developed to enhance the interfacial bonding strength (Ref 5), but the high brazing temperature and the existence of Ni as the catalyst usually led to the degradation of diamond during brazing operation (Ref 14). Accordingly, Cu-based alloys, such as Cu-10Sn-15Ti, have been presented as ideal brazing alloys for diamond, in which Ti is an active metal and Sn is a melting temperature depressor. A brazing temperature lower than 950 °C can be applied to this alloy, and, due to the lack of catalyst for the degradation of diamond and the development of an interfacial TiCx layer during brazing operation, the degradation of diamond can be retarded and the bonding strength can be enhanced (Ref 14-16). For example, the bonding strength between Cu-20Sn-10Ti and diamond was about 344 MPa, evaluated by a tensile test using a Houndsfield tensometer (Ref 2). Such a bonding strength value was very close to the flexural strength of CVD diamond (370 MPa) (Ref 17). The other groups of brazing alloys are Ag-based alloys, with the addition of Cu as the melting temperature depressor and a small quantity of Ti as the active metal. These Ag-based alloys have lower brazing operation temperatures than the Cu-based brazing alloys, but the concerns with the high cost, the low active metal concentration, and the low yield strengths of these alloys may limit their widespread application (Ref 3).

Though the above-mentioned alloys were widely used in brazing diamond, most efforts in these studies were focused on the phase development, especially that near the bonding interface. The bonding strength between a brazing alloy and diamond is generally ignored, not to mention a direct comparison of bonding strength among different brazing alloys. In this study, the above-mentioned three groups of brazing alloys are compared, including two Ni-based, one Cu-based, and two Ag-based alloys. Two CVD diamond slabs were brazed together into a brazed joint, with the brazing alloy lying between them. The surface of the CVD diamond near the brazed side was analyzed subsequent to brazing operation. The bend strength of the brazed joint, determined by a four-point bending test, was compared with the flexural strength of CVD diamond (Ref 17) and the fracture path was examined. The optimal brazing operation was then identified and the guidelines to the design of brazing alloys were concluded.

Yu-Chan Hsieh and **Shun-Tian Lin**, Department of Mechanical Engineering, National Taiwan University of Science and Technology, 43 Keelung Road, Sec. 4, Taipei 106, Taiwan, ROC. Contact e-mail: D9303501@mail.ntust.edu.tw.

2. Experimental

Five different brazing alloys were used in this study, including two nickel-based, one copper-based, and two silver-based alloys. The nickel-based alloy powders (Höganäs, HBNi2 and HBNi7) were produced by gas atomization, whose mean particle sizes were about 106 μm. A copper-based powder, Cu-10Sn-15Ti (wt.%), was produced by gas-atomization, whose mean particle size was about 24 μm. The silver-based brazing alloys were received in the foil state, with thicknesses of 0.1 mm (ABA, Silver ABA) and 0.08 mm (ABA, Cusin-1-ABA), respectively. The compositions of these five different brazing alloys are shown in Table 2.

Table 1 A compilation of various Ni-, Cu-, and Ag-based alloys that were used to braze diamond in the literatures (Ref 1, 2, 4-12)

Group	Composition, wt.%	Brazing temperature, °C	Reference
Ni-based	Ni-14Cr-10P	1000	1
	Ni-7Cr-2.9B-4.5Si-3Fe-0.1C	1100	4
	Ni-13.5Cr-3B-4.25Si-4.75Fe-0.75C	1100	4
	Ni-26Cr-4Si-3.3B-1Fe-0.95C	1120	4
	Ni-19.5Cr-9.6Si-9.5Mn	1160	4
	Ni-10Cr-3.5Si-2B	1050	5
	Ni-12Cr-4Fe-3Si-2.5B	1000	6
	Ni-14.4Cr-3.5Fe-3.5Si-3.35B	1080	11
	Ni-14.3Cr-3.5Fe-3.5Si-3.2B	1080	12
Cu-based	Cu-20Sn-10Ti	900-1150	2
	Cu-20Sn-2.1Ti	900-1150	2
	Cu-14.4Sn-10.2Ti-1.5Zr	930	8
Ag-based	Ag-34.5Cu-1.5Ti	810-850	7
	92(72Ag-28Cu)-8Ti	850-970	9
	Ag-27.25Cu-12.5In-1.25Ti	740	10

Table 2 Compositions and brazing temperatures of the brazing alloys used in this study

Brazing alloys	Composition, wt.%	Brazing temperature, °C
HBNi2	Ni-3Fe-7Cr-3B-0.5Si-0.02C	1030
HBNi7	Ni-14Cr-10P-0.02C	1030
Cu-Sn-Ti	Cu-10Sn-15Ti	950
Silver ABA	Ag-5Cu-1Al-1.25Ti	950
Cusin-1-ABA	Ag-34.25Cu-1In-1.75Ti	850

Two CVD diamond blocks of 5 × 5 × 2 mm in dimension, fabricated by microwave plasma deposition, were brazed together side by side using either one of the brazing alloys as the filler between the blocks. An illustration of the brazing arrangement is shown in Fig. 1. For the brazing powders, powder pastes were prepared using water solution of starch (20 vol.%) as the binder, and the pastes were individually filled in the gap between the diamond blocks. On the other hand, the brazing foils were cut to the exact dimension and filled in the gap between the diamond blocks. A graphite fixture was used to firmly fix the to-be-brazed structure. A mass of 50 g was applied to the diamond side during brazing, as indicated in Fig. 1(b), in order to avoid distortion of the brazed structure. Brazing was carried out in a high vacuum furnace, using graphite as the heating element and heat shield, with a vacuum better than 1×10^{-5} Torr. The temperature profiles included a ramp of 10 °C/min to the brazing temperature, which ranged between 850 and 1030 °C, depending on the alloy composition (Table 2). The isothermal holding time at the brazing temperature was 15 min.

After brazing, the graphite fixture was removed by grinding using a SiC sand paper. A four-point bending test was carried out for the brazed joints at a crosshead speed of 5 mm/min. The fixture for this test is shown in Fig. 2. X-ray diffraction (XRD, RIGAKU DMAX-VB) patterns of the brazing alloys were recorded, using Cu K_α. The operating voltage was 40 kV, and a scanning interval of 0.02° was carried out at a scanning rate of 5°/min in the range of 2θ = 30-80°. Subsequently, the brazing alloys were leached away using aqua regia and the precipitated phases on diamond surface were analyzed using scanning electron microscope (SEM, JEOL JSM-T330A). Secondary electron image (SEI) and electron dispersive X-ray spectroscopy (EDS) were recorded at an accelerating voltage of 20 kV. The integrity of diamond before and after brazing operation was analyzed using Raman spectroscopy (JOBIN YVON HORIBA HR800UV, Nd-YAG laser type: λ = 514 nm).

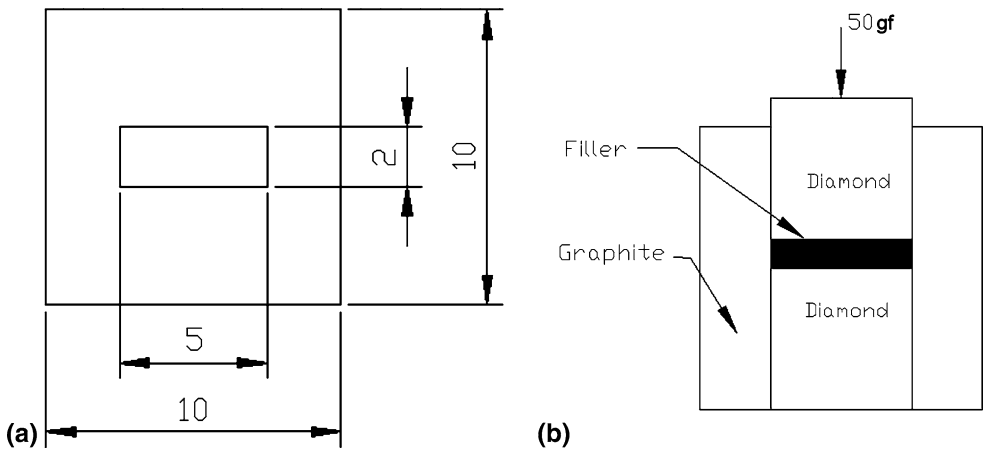

Fig. 1 Illustration of specimen dimensions in brazing: (a) top view and (b) front view

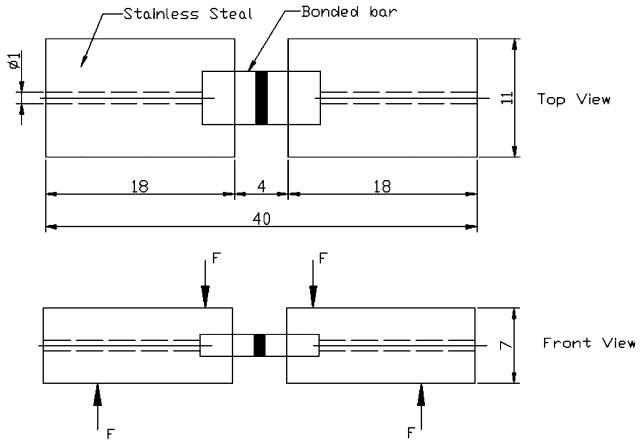

Fig. 2 Setup of four-point bending test

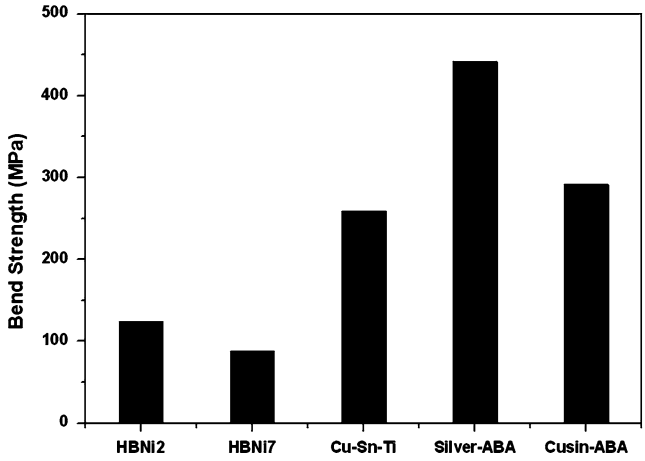

Fig. 3 Bend strengths of five brazed joints using different brazing alloys

3. Results and Discussion

Figure 3 shows the bend strength of the brazed joint. Both of the nickel alloys exhibited very low bend strengths (124 and 88 MPa). The bend strength for the brazed joint using Cu-10Sn-15Ti as the brazing alloy was 260 MPa, which was lower than the fracture strength of this alloy, because this alloy was dispersion-hardened by many precipitated intermetallic compounds (Ref 16). Indeed, this alloy had been demonstrated in various occasions which showed an excellent brazing performance on diamond grits (Ref 14-16). Accordingly, it was expected that the fracture path took place primarily along the weakest interface between the brazing alloy and the CVD diamond for the above-mentioned three brazing alloys. On the other hand, both of the silver-based alloys yielded high bend strengths (442 and 291 MPa), with Ag-5Cu-1Al-1.25Ti having a highest bend strength. Such a bend strength, 442 MPa, is similar in order to or even higher than the bend strength of CVD diamond, which ranges between 261 and 984 MPa (Ref 17). Accordingly, the fracture path might have propagated through the CVD diamond instead of the interface between the brazing alloy and the CVD diamond.

Figure 4 shows the XRD patterns for the brazing alloys before and after brazing operation. There were slight changes in constituting phases in each alloy before and after brazing operation. It can be observed that HBNi2 (Ni-3Fe-7Cr-3B-4.5Si-0.02C) in the as-received state could exist in an amorphous state or at least a highly strained lattice (Ref 18). It developed into Ni-based alloys, ternary NiSiB and CrNiSi compounds after brazing operation. HBNi7 (Ni-14Cr-10P-0.02C) was initially composed of various complex phases but developed into simply Ni_3P-based phase. The gas-atomized Cu-10Sn-15Ti prealloyed powder experienced minor phase changes in the dispersed intermetallic phases after brazing operation, from Sn_3Ti_5 and Sn_3Ti_5 into $SnTi_3$, $CuTi_2$, and $CuSn_3Ti_5$ (Ref 15). The silver-based alloys (Ag-5Cu-1Al-1.25Ti and Ag-34.25Cu-1In-1.75Ti) did not experience too much change in their constituting phases after brazing operation, probably due to the low concentrations of the alloying elements.

Figure 5 shows the SEI images near the diamond side, after leaching the brazing alloys with aqua regia ($3HCl + 1HNO_3$). Figure 5(a) shows that the brazing alloy (HBNi2, Ni-3Fe-7Cr-3B-4.5Si-0.02C) had been completely leached away from the

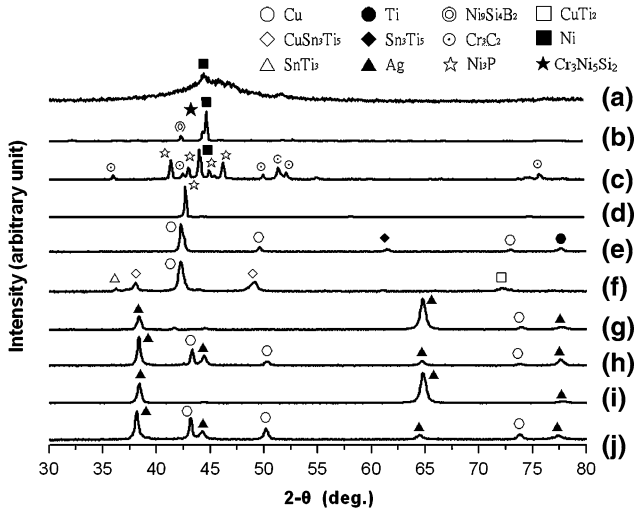

Fig. 4 XRD patterns before and after brazing operation for (a) HBNi2 filler, (b) as-brazed HBNi2, (c) HBNi7 filler, (d) as-brazed HBNi7, (e) Cu-Sn-Ti filler, (f) as-brazed Cu-Sn-Ti, (g) Silver-ABA filler, (h) as-brazed Silver-ABA, (i) Cusin-ABA filler, and (j) as-brazed Cusin-ABA

CVD diamond surface. Compositional analysis based on EDS indicated that no other element than C was left behind on the surface of the CVD diamond surface. Accordingly, the possible carbide phase that formed on the diamond surface was believed to weakly bond to diamond, which was leached away from the diamond surface along with the matrix (Ref 14). Figure 5(b) shows the chromium carbide that was left behind on the CVD diamond surface, when (HBNi7, Ni-14Cr-10P-0.02C) was used as the brazing alloy. Compositional analysis based on EDS indicated that its composition was very close to Cr_3C_2, which initially existed in the as-received powder but disappeared from the matrix, as indicated in the XRD patterns shown in Fig. 4(c) and (d). The Cr_3C_2 phase, which had an orthorhombic structure, was discretely dispersed on the surface of CVD diamond, which was quite different from what was observed for Cu-Sn-Ti alloy where a continuous interfacial TiCx film formed

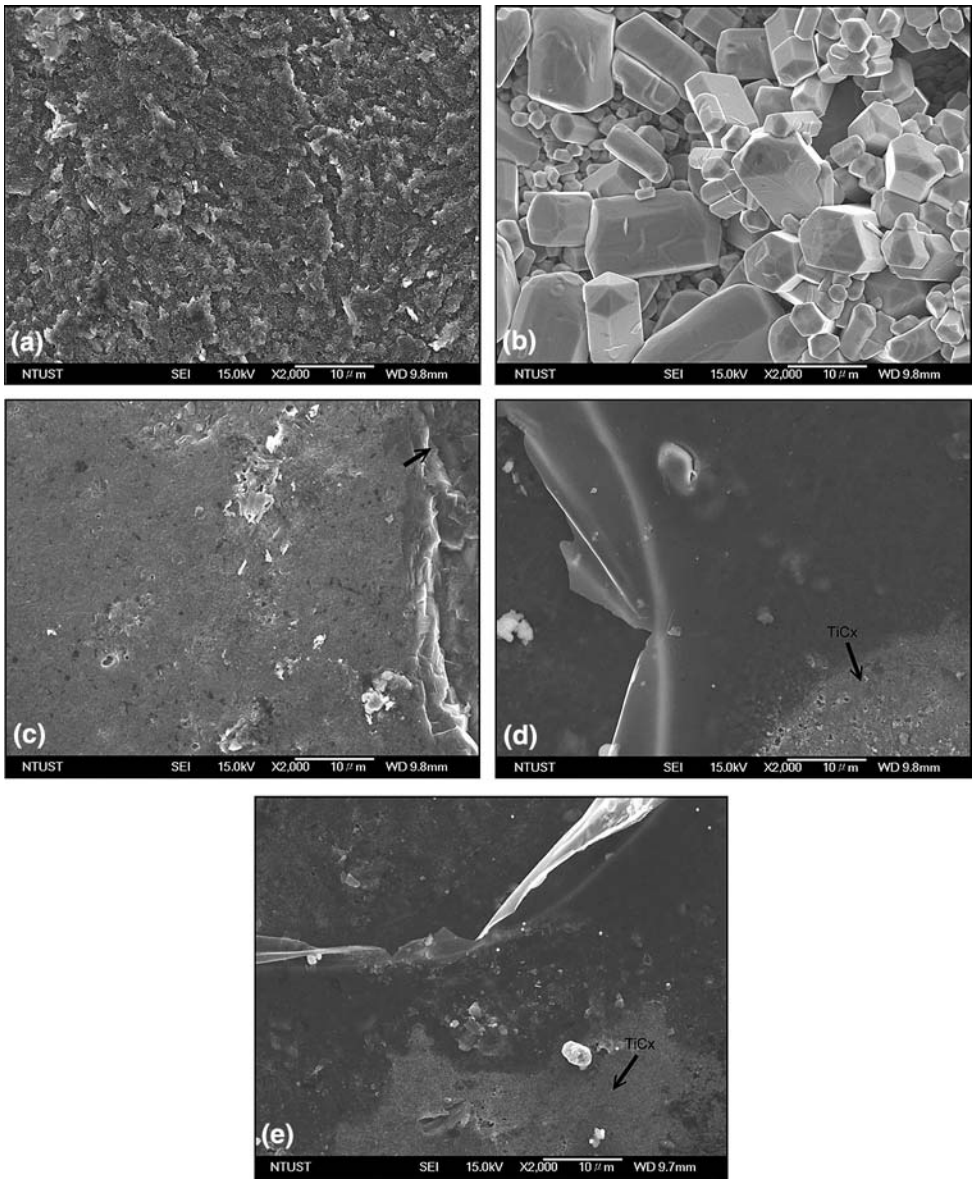

Fig. 5 SEI images near the diamond side after the brazing alloys were leached away from the brazed joints using aqua regia: (a) HBNi2, (b) HBNi7, (c) Cu-Sn-Ti, (d) Silver-ABA, and (e) Cusin-ABA

on the surface of diamond (Ref 16). The continuous TiCx film not only could retard the degradation of diamond (indicated by the arrow of Fig. 5c), but also enhance the bend strength between the brazing alloy and the CVD diamond, as shown in Fig. 3. The surfaces of CVD diamond after brazing practice using Cu- and Ag-based brazing alloys that contained Ti were very intact, compared with that using HBNi2 (Ni-3Fe-7Cr-3B-4.5Si-0.02C) as the brazing alloy (Fig. 5a). Indeed, traced amount of Ti could be found on the diamond surface, implying that TiCx was strongly bonded to diamond (Ref 19). The interfacial TiCx layer played a key role in the transition from a highly covalent bond structure (diamond) to metallic bond structure (Cu alloys or Ag alloys), and alleviated the stress associated with dissimilar bonding structures.

Figure 6 shows the Raman spectra of diamond before and after the brazing operation, with those after brazing operation being examined on the brazed surface. The as-received CVD diamond had a broad but weak sp^2 bond peak near 1580 cm^{-1}, in addition to a sharp and strong sp^3 peak near 1333.5 cm^{-1}. This observation indicated that this CVD diamond was not diamond of high quality. Indeed, it looked opaque. With HBNi2 (Ni-3Fe-7Cr-3B-4.5Si-0.02C) as the brazing alloy, the CVD diamond near the brazed surface severely transformed into sp^2-bonded carbon after brazing operation, which was responsible for the rugged surface observed in Fig. 5(a). Similarly, with HBNi7 (Ni-14Cr-10P-0.02C) as the brazing alloy, the CVD diamond near the brazed surface transformed into sp^2-bonded carbon after brazing operation, but not as severe as that observed when HBNi2 was used as the brazing alloy. Indeed, the higher Cr concentration in HBNi7 alloy than in HBNi2 caused the formation of abundant Cr_3C_2 grains near the interface between the brazing alloy and the CVD diamond

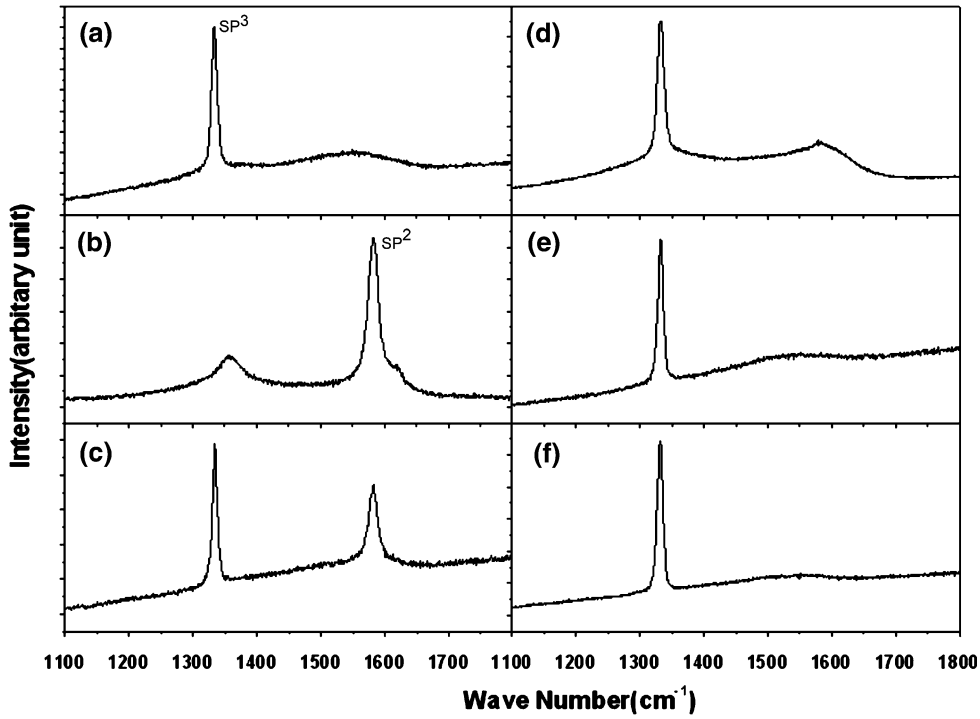

Fig. 6 Raman spectra of (a) as-received CVD Diamond, and the CVD diamond after brazing operation using (b) HBNi2, (c) HBNi7, (d) Cu-Sn-Ti, (e) Silver-ABA, or (f) Cusin-ABA as the brazing alloy

(Fig. 5b), which more effectively retarded the further catalyzed transformation of diamond into sp^2-bonded carbon by Ni. With Cu-15Sn-10Ti as the brazing alloy, there was slight transformation of diamond into sp^2-bonded carbon, probably due to the high concentration of Ti in the alloy. On the other hand, with the Ag-based brazing alloys that contained much lower concentrations of Ti, the quality of the CVD diamond could be effectively retained. Accordingly, though Ti in the Cu- and Ag-based alloys could retard the degradation of diamond by forming an interfacial TiCx layer, it was also a catalyst for the transformation of diamond into sp^2-bonded carbon.

Figure 7 shows the representative fractured surfaces for the brazed joint using different brazing alloys, and Fig. 8 shows the illustrative fracture paths observed from a series of fracture surfaces similar to those shown in Fig. 7. For the two Ni-based brazing alloys, the crack propagated primarily along the interface between the CVD diamond and the brazing alloy, where either sp^2-bonded carbon or the discrete Cr_3C_2 grains near the brazed interface was the weakest path. With Cu-10Sn-15Ti as the brazing alloy, the brazed joint fractured primarily through the brazing alloy bulk. This observation indicated that the fracture strength of the brazing alloy bulk was much lower than that of the interface between the CVD diamond and the brazing alloy. The development of a thin TiCx layer in the interface effectively enhanced the interfacial bonding strength by alleviating the stress arising from differences in bond type and lattice parameter and phase transformation of the brazing alloy during cooling, though with a minor trend toward transforming the CVD diamond into sp^2-bonded carbon. The weak brazing alloy bulk could have arisen from the precipitation of various intermetallic compounds of large quantity in the alloy, due to the high concentrations of Sn and Ti in the alloy (Ref 15). The formation of abundant brittle intermetallic compounds in a Cu-based matrix led the fracture path propagating mainly through the alloy bulk. With the two silver-based brazing alloys, the cracks propagated either in the CVD diamond bulk or along the brazed interface, implying that both the brazed interface and the brazing alloy bulk were very strong. Based on the above observations, it can be concluded that Cu- and Ag-based alloys with low concentrations of Ti are the ideal alloys for brazing diamond.

4. Conclusion

The phase development near the interface between the CVD diamond and the brazing alloy dictated the bond strength of the brazed joint. The Ni-Cr alloys using either B or P as the melting point depressor caused the catalytic degradation of diamond into sp^2-bonded carbon after brazing operation. Fracture propagated along the brazed interface under a low stress. With Cu-10Sn-15Ti as the brazing alloy, the brazed interface was stronger than the brazing alloy bulk and the brazed joint cracked through the brazing alloy bulk, due to the high concentrations of Sn and Ti in the alloy that caused the precipitation of abundant intermetallic compounds in the brazing alloy bulk. On the other hand, the active metal Ti in the Ag-based alloys was very low in concentration. The strength of the brazing alloy bulk was high and high stresses were needed to break the brazed joints, whose fracture paths were either along the brazed interface or even across the CVD diamond.

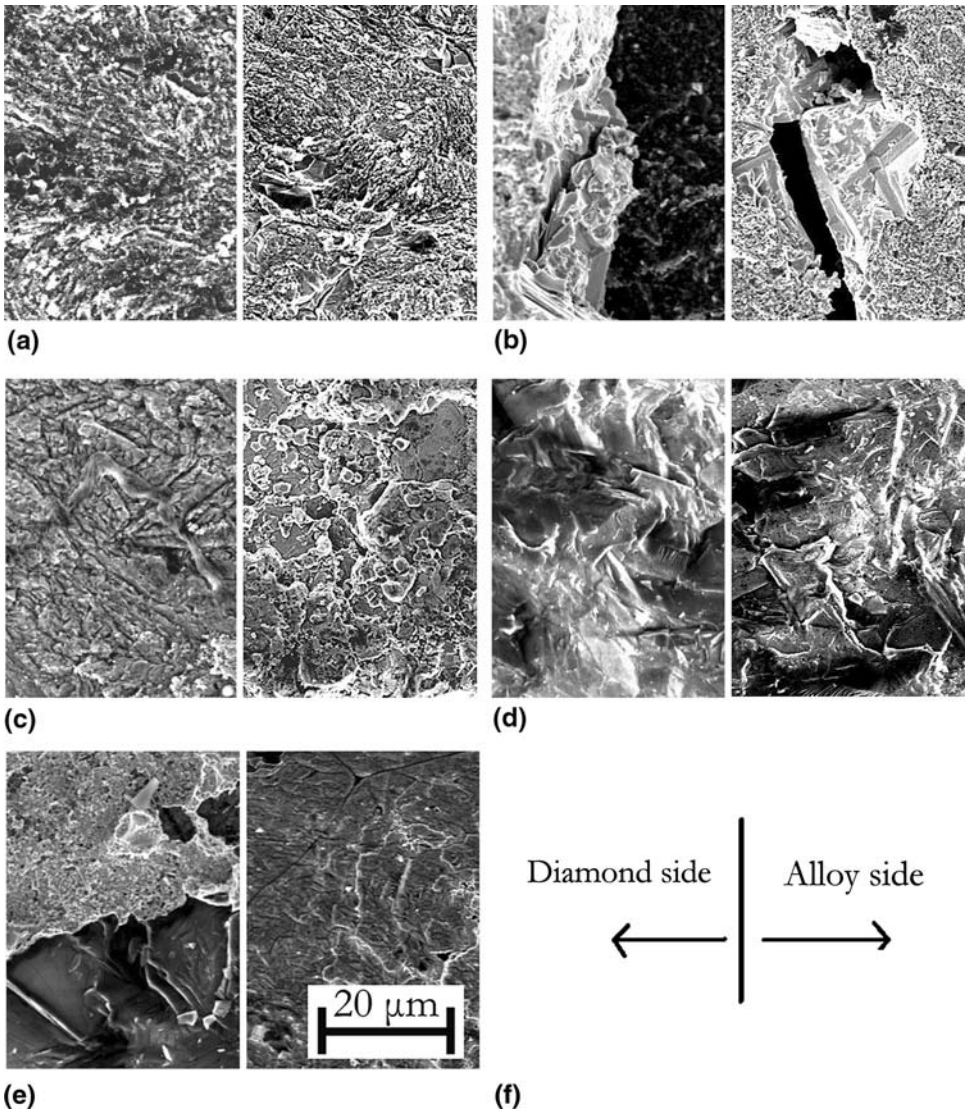

Fig. 7 Fractured surfaces for the brazed joint using (a) HBNi2, (b) HBNi7, (c) Cu-Sn-Ti, (d) Silver-ABA, or (e) Cusin-ABA as the brazing alloy

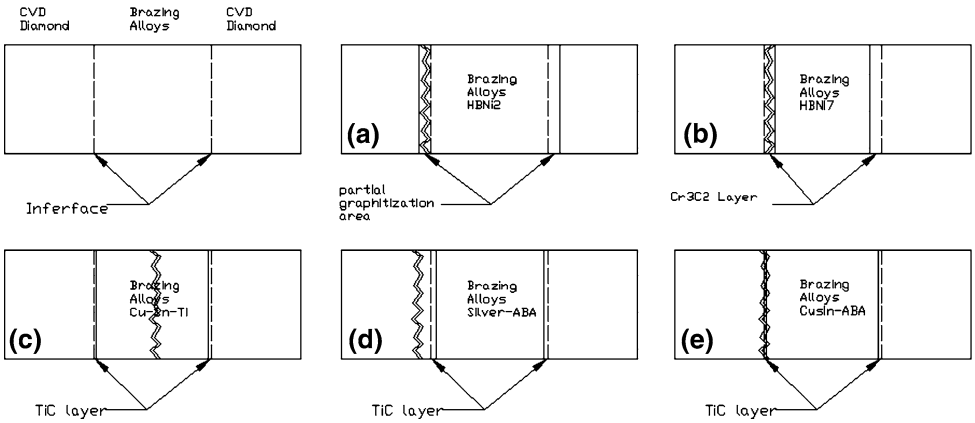

Fig. 8 Illustration of fractured path for the brazed joint using (a) HBNi2, (b) HBNi7, (c) Cu-Sn-Ti, (d) Silver-ABA, or (e) Cusin-ABA as the brazing alloy

References

1. A.K. Chattopadhyay and H.E. Hintermann, On Brazing of Cubic Boron Nitride Abrasive Crystals to Steel Substrate with Alloys Containing Cr or Ti, *J. Mater. Sci.*, 1993, **28**, p 5887
2. D. Evens, M. Nicholas, and P.M. Scott, The Wetting and Bonding of Diamonds by Copper-Tin-Titanium Alloys, *Ind. Diamond Rev.*, 1977, **37**, p 306
3. T. Yamazaki and A. Suzumura, Role of the Reaction Product in the Solidification of Ag-Cu-Ti Filler for Brazing Diamond, *J. Mater. Sci.*, 1998, **33**, p 1379
4. J.T. Loefrt and E.M. Tausch, Method of Manufacturing Diamond Abrasive Tools, U.S. Patent 3894673, 1975
5. Z.J. Yao, H.H. Su, Y.C. Fu, and H.J. Xu, High Temperature Brazing of Diamond Tools, *Trans. Nonferr. Metall. Soc. China*, 2005, **15–16**, p 1227
6. S.F. Huang, H.L. Tsai, and S.T. Lin, Effects of Brazing Route and Brazing Alloy on the Interfacial Structure Between Diamond and Bonding Matrix, *Mater. Chem. Phys.*, 2004, **84**, p 251
7. A. Palavra, A.J.S. Fernandes, C. Serra, F.M. Costa, L.A. Rocha, and R.F. Silva, Wettability Studies of Reactive Brazing Alloys on CVD Diamond Plates, *Diamond Relat. Mater.*, 2001, **10**, p 775
8. F.A. Khalid, U.E. Klotz, H.R. Elsener, B. Zigerlig, and P. Gasser, On the Interfacial Nanostructure of Brazed Diamond Grits, *Scripta Mater.*, 2004, **50**, p 1139
9. F. Sun, J. Feng, and D. Li, Bonding of CVD Diamond Thick Films Using an Ag-Cu-Ti Brazing Alloy, *J. Mater. Process. Technol.*, 2001, **115**, p 333
10. U.E. Klotz, F.A. Khalis, and H.R. Elsener, Nanocrystalline Phases and Epitaxial Interface Reactions During Bazing of Diamond Grits with Silver Based Incusil-ABA Alloy, *Diamond Relat. Mater.*, 2006, **15**, p 1520
11. A.K. Chattopadhyay, L. Chollet, and H.E. Hintermann, Induction Brazing of Diamond with Ni-Cr Hardfacing Alloy Under Argon Atmosphere, *Surf. Coat. Technol.*, 1991, **45**, p 293
12. A.K. Chattopadhyay, L. Chollet, and H.E. Hintermann, Experiment Investigation on Induction Brazing of Diamond with Ni-Cr Hardfacing Alloy Under Argon Atmosphere, *J. Mater. Sci.*, 1991, **26**, p 5093
13. A. Rabinkin, E. Wenski, and A. Ribaudo, Brazing Stainless Steel Using a New MBF-Series of Ni-Cr-B-Si Amorphous Brazing Foils, *Weld. World*, 1998, **41**, p 466
14. S.F. Huang, H.L. Tsai, and S.T. Lin, Laser Brazing of Diamond Grits Using a Cu-15Ti-10Sn Brazing Alloy, *Mater. Trans. JIM*, 2002, **43**(10), p 2604
15. W.C. Li, C. Liang, and S.T. Lin, Interfacial Segregation of Ti in the Brazing of Diamond Grits onto a Steel Substrate Using a Cu-Sn-Ti Brazing Alloy, *Metall. Mater. Trans. A*, 2002, **33A**, p 2163
16. W.C. Li, C. Liang, and S.T. Lin, Epitaxial Interface of Nanocrystalline TiC Formed Between Cu-10Sn-15Ti Alloy and Diamond, *Diamond Relat. Mater.*, 2002, **11**, p 1366
17. K.L. Jackson, D.L. Thurston, P.J. Boudreaus, R.W. Armstrong, and C.C. Wu, Fracturing of Industrial Diamond Plates, *J. Mater. Sci.*, 1997, **32**, p 5035
18. A.M. Hadian and R.A.L. Drew, Thermodynamic Modeling of Wetting at Silicon Nitride/Ni-Cr-Si Alloy Interfaces, *Mater. Sci. Eng. A*, 1994, **189**, p 209
19. Y.Z. Hsieh and S.T. Lin, Diamond Tool Bits with Iron Alloys as the Binding Matrices, *Mater. Chem. Phys.*, 2001, **72**, p 121